


An *In Vivo* Lapine Model for Impact-Induced Injury and Osteoarthritic Degeneration of Articular Cartilage

Cartilage
3(4) 323–333
© The Author(s) 2012
Reprints and permission:
sagepub.com/journalsPermissions.nav
DOI: 10.1177/1947603512447301
http://cart.sagepub.com


Peter G. Alexander¹, Jesse A. McCarron², Matthew J. Levine², Gary M. Melvin³, Patrick J. Murray², Paul A. Manner², and Rocky S. Tuan¹

Abstract

Objective: In this study, we applied a spring-loaded impactor to deliver traumatic forces to articular cartilage *in vivo*. Based on our recent finding that a 0.28-J impact induces maximal catabolic response in adult bovine articular cartilage *in vitro* using this device, we hypothesize that this impact will induce the formation of a focal osteoarthritic defect *in vivo*. **Design:** The femoral condyle of New Zealand White rabbits was exposed and one of the following procedures performed: 0.28 J impact, anterior cruciate ligament transection, articular surface grooving, or no joint or cartilage destruction (control). After 24 hours, 4 weeks, or 12 weeks ($n = 3$ for each time point), wounds were localized with India ink, and tissue samples were collected and characterized histomorphometrically with Safranin O/Fast green staining and Hoechst 33342 nuclear staining for cell vitality. **Results:** The spring-loaded device delivered reproducible impacts with the following characteristics: impact area of $1.39 \pm 0.11 \text{ mm}^2$, calculated load of $326 \pm 47.3 \text{ MPa}$, time-to-peak of $0.32 \pm 0.03 \text{ ms}$, and an estimated maximal displacement of $25.1\% \pm 4.5\%$ at the tip apex. The impact resulted in immediate cartilage fissuring and cell loss in the surface and intermediate zones, and it induced the formation of a focal lesion at 12 weeks. The degeneration was defined and appeared more slowly than after anterior cruciate ligament transection, and more pronounced and characteristic than after grooving. **Conclusion:** A single traumatic 0.28 J impact delivered with this spring-loaded impactor induces focal cartilage degeneration characteristic of osteoarthritis.

Keywords

articular cartilage, mechanical impact, trauma, cartilage degeneration, osteoarthritis, *in vivo* model

Introduction

Osteoarthritis is a painful, disabling disease of synovial joints, characterized by erosion of articular cartilage, osteophyte formation, increases in subchondral bone mass and subchondral bone cysts.¹ Histologically, advanced osteoarthritis involves changes in matrix composition, including net loss of collagen type II and aggrecan, decrease in tissue cellularity, progressive fissuring, pannus formation, and vascular invasion.² The disease progresses because of a gradually increasing imbalance between anabolic and catabolic processes required for normal tissue homeostasis.^{3–6} The main functions of the articular cartilage are mechanical—to allow frictionless motion and to absorb and distribute loads. Forces outside the physiological range or an intrinsic inability of the articular cartilage to manage normal loads are sufficient to initiate osteoarthritis.^{7,8}

Animal models have been developed to study the role of mechanical disruptions such as trauma, instability, and wear in osteoarthritis pathogenesis.^{9,10} Noninvasive wear models

are most physiological, but the time and location of disease onset are unpredictable and imprecise and the forces responsible are difficult to define. Instability and chondral defect models, such as anterior cruciate transection, debridement, and microfracture, have similar experimental complications and introduce forces and factors that do not replicate most osteoarthritic pathogenesis in the human condition.¹¹ Impact

¹Department of Orthopaedic Surgery, University of Pittsburgh, Pittsburgh, PA, USA

²Department of Orthopaedic Surgery, George Washington University, Washington, DC, USA

³Office of Science and Technology, National Institute of Arthritis, and Musculoskeletal and Skin Diseases, National Institutes of Health, Bethesda, MD, USA

Corresponding Author:

Rocky S. Tuan, PhD, Director, Center for Cellular and Molecular Engineering, Department of Orthopaedic Surgery, University of Pittsburgh, 450 Technology Drive, Room 221, Pittsburgh, PA 15219, USA
Email: rst13@pitt.edu

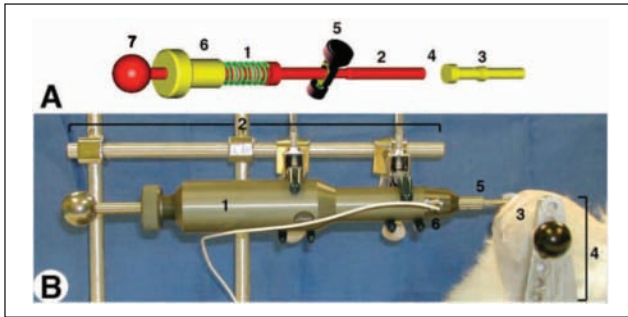


Figure 1. (A) Impactor schematics. The compression of the spring in the load mechanism (A1) is controlled by the threaded screw (A6; 1 mm compression/360° of turn) mated with the housing of the impactor (not shown). Thus, the force applied to the missile on spring release is linearly related to the turns of the screw. Compression is accomplished by pulling the tensor knob (A7) until the release mechanism (A5) engages a notch in the piston. Activating the release mechanism (A5) releases the piston (A2) that collides with the interchangeable impactor missile (A3), which ultimately strikes the cartilage. The internal load cell (A4) is placed in-line between the piston (A2) and missile (A3), and fixed to the latter. There is sufficient travel between the piston and projectile so that the piston does not contact the missile at the time of cartilage impact. (B) Setup for ex vivo impact of 5-mm cartilage plugs. (B) Setup for in situ impact showing the completed impactor (B1) in a fixed armature (B2) with a hemispherical tip (B5) in contact with the left stifle, medial femoral condyle (B3) of a New Zealand White rabbit (euthanized) placed in its own armature (B4) contiguous with that of the impactor, and signal lead (B6) of internal load cell.

models promise the application of a defined mechanical insult at a specific time and place to permit the study of osteoarthritis pathogenesis. The applications of defined loads *in vivo* that induce osteoarthritic changes have been difficult and infrequent with notable exceptions.¹²⁻¹⁸ The greatest challenge has been to quantify the impact in magnitude, speed, and area, and to characterize the pathogenesis of the osteoarthritic condition following the injury.

Previous impact model studies have often used young, skeletally immature animals. However, cellular and matrix alterations occur during aging and are correlated with inferior mechanical performance of articular cartilage.¹⁹ These alterations may increase the susceptibility of the tissue to traumatic forces and are likely to be relevant to the development of osteoarthritis in humans. The goal of this study was to develop a consistent, reproducible, adult small animal model to study the onset and early pathogenesis of posttraumatic osteoarthritis in middle-aged animals.

Materials and Methods

A custom-engineered, spring-loaded impactor (**Fig. 1A**) was designed to deliver 100 to 2000 N using interchangeable springs and a smooth, stainless steel hemispherical tip

Table 1. Induction of Key Markers of Early Cartilage Damage After Impact in an *In Vitro* Study Using Adult Bovine Articular Cartilage

Markers of cartilage damage	17-MPa impact (%)	36-MPa impact (%)
Cell death ^a	22 ± 5	53 ± 9
GAG release ^a	218 ± 42%	309 ± 34
NO release ^a	256 ± 78	605 ± 135
PGE2 release ^a	183 ± 41	424 ± 111
MMP with increased expression ^a	MMP9, MMP13	MMP3, MMP9

Note: GAG = glycosaminoglycan; NO = nitric oxide; PGE2 = prostaglandin E2; MMP = matrix metalloproteinase.

^aCompared with control levels of cartilage damage marker.

with a radius of 2.5 mm. The compression of the 5-mm spring in the load mechanism is controlled by the threaded screw (1 mm compression/turn) mated with the housing of the impactor (**Fig. 1A**). Thus, the force applied to the missile on spring release is linearly related to the turns of the screw. A critical element of the device design is that sufficient travel between the piston and projectile is allowed so that the piston does not contact the missile at the time of cartilage impact. Although originally intended for handheld use, a fixation device was added to clamp the impactor and an *ex vivo* sample chamber to create a rigid system (**Fig. 1B**). Impact forces were recorded with two 10 to 200 lb quartz force sensors (QFG 200, Cooper Instruments, Warrendale, VA) fitted in-line between the internal piston and impactor projectile (**Fig. 1A**). Force profiles were sampled at 200 kHz using a signal conditioner model QSC 484 (Cooper Instruments), an analog-to-digital converter model NI-9215 (BNC-USB; National Instruments Corp., Austin, TX) and LabView 7.0 software (National Instruments). Force curves were analyzed in Microsoft Excel (Redmond, WA). Impact area, defined as the maximum tissue surface area contacted by the hemispherical projectile tip during an impact motion, was measured using medium sensitivity Fuji Presssurex pressure-sensitive film (Sensor Products, Inc., East Hanover, NJ) placed between the impactor tip and the articular surface. Impact footprints were digitally scanned using a Microtek flatbed scanner, rendered in Adobe Photoshop CS2 (Adobe, San Jose, CA) and analyzed for geometry using NIH ImageJ 1.62.

Based on our recent findings, we determined that a 36-MPa impact using the novel spring-loaded device described above induced a reproducibly damaging impact to adult bovine articular cartilage of the patellofemoral groove. This impact induced maximal levels of cell death, release of sulfated glycosaminoglycans nitric oxide, and prostaglandin E2, as well as the expression of specific matrix metalloproteinases (**Table 1**). The impact was found to be traumatic in nature, characterized by a rise-to-maximum load time less than 2 ms (0.47 ± 0.02 ms), a loading

Table 2. Comparison of Impact Characteristics Delivered Using a Spring-Loaded Impactor on Bovine Cartilage *In Vitro* and Lapine Cartilage *In Vivo*^a

	Impact area (mm ²)	Time to peak (ms)	Peak force (N)	Normalized peak impact stress (MPa)	Maximum displacement (%)	Spring potential energy (J)	Loading rate to peak force ($\times 10^3$ N/s)	Average stress rate ($\times 10^3$ MPa/s)	Average strain rate ($\times 10^3$ %/s)
<i>In vitro</i> (adult bovine articular cartilage)	12.6 \pm 2.7	0.47 \pm 0.02	453.52 \pm 82.1	36.05 \pm 5.62	38.55 \pm 3.54	0.27783	970.44 \pm 81.81	77.14 \pm 5.62	82.50 \pm 3.54
<i>In vivo</i> (adult lapine articular cartilage)	1.39 \pm 0.11	0.32 \pm 0.04	236 \pm 95.2	169 \pm 68.4	21.5 \pm 4.5	0.27783	737.5 \pm 182	528.1 \pm 69	67.2 \pm 4.6

^aImpacts delivered using a 9-mm spring compression setting (0.28 J) and a mass of 220 g. *In vitro*: adult bovine patellofemoral groove articular cartilage without subchondral bone. *In vivo*: adult lapine articular cartilage of the medial femoral condyle.

rate of rise-to-peak force of 970×10^6 N/s, and an average stress rate of $77.14 \pm 5.62 \times 10^3$ MPa/s (Table 2). The 36-MPa setting was used for all impacts in this study. As described below, impacts were performed *in situ* with both the right knee and impactor locked in a rigid armature. In addition, the disease progression of the impact model is compared with that of an anterior cruciate ligament transection (ACLT) or groove model.

In Vivo Impact and Osteoarthritis Development

Thirty-six New Zealand White rabbits aged 18 to 24 months (retired breeders; Covance, Gaithersburg, MD) underwent survival surgery to their right knee via a medial parapatellar arthrotomy. All animals were anesthetized and laid on a heated pad. The left hind stifle was mounted on a fixed, aluminum armature of 2 vertical posts that held 2 parallel bars height-adjustable to compensate for the size of the animal. The hind stifle was stretched such that the knee was above the upper bar. The knee was flexed to position the ankle behind the lower bar. In this position, the knee was flexed approximately 145° to 160°. The knee was pressed tightly against the upper rod such that no additional fixation was required. After the medial parapatellar approach, the impactor tip was positioned immediately above the articular cartilage of the medial femoral condyle in the most posterior location possible with this approach. Polyethylene encased pressure-sensitive paper was placed between the cartilage and impactor tip. The impact was then delivered by releasing the spring. In a separate group of animals, ACLT was accomplished using a small iris scissors in the left knee of the hind stifle as a model of instability,²⁰ or articular surface defect was produced by fitting a 1-mm radius burr to a pneumatic drill.²¹ A 3- to 4-mm long region of articular cartilage on the medial femoral condyle was removed. Care was taken to avoid violating the subchondral bone. A separate set of animals was used for sham control. Postoperative radiographs confirmed that the subchondral bone was not fractured or significantly violated. Animals were then sacrificed at 24 hours, 4 weeks, or 12 weeks. During the postoperative period, animals were caged in pairs, given appropriate enrichment and encouraged to run and play in a

polyvinyl carbonate children's pool for 1 hour each day. Hopping was considered critical since extension was required for the impacted area to experience physiological loads.

Histological Analysis

After sacrifice, both the impacted knee and uninjured contralateral control knees were fixed in 4% paraformaldehyde, rinsed in phosphate-buffered saline, stained with India ink, and photographed with a Qimaging Micropublisher 5.0 CCD color camera (Bumbay, BC, Canada) mounted on a Leica MZF1 III dissecting microscope. Five weightbearing areas per knee were isolated and processed for histology: the injury site, an uninjured, neighboring region of the medial femoral condyle, a portion of the medial tibial plateau, and corresponding surfaces from the lateral femoral condyle and lateral tibial plateau. All tissue samples were decalcified in Immunocal (Decal Chemical Corp., Tallman, NY) for 14 days at 4 °C and paraffin embedded. Specimens were sectioned perpendicular to the articular cartilage surface at 8 μ m thickness and stained with Safranin-O/Fast Green, hematoxylin/eosin, or Hoechst 33342 fluorescent nucleic acid stain according to the manufacturer's protocols (Molecular Probes, Eugene, OR). Quantification of cell loss was accomplished through image processing in ImageJ and involved the counting of Hoechst 33342 stained nuclei (characteristic of viable cell nuclei) in 3 randomly chosen regions of fixed area in the impact zone. All chemicals were purchased from Sigma (St. Louis, MO) unless specified otherwise. Cartilage depth from surface to tidemark was measured microscopically at regions adjacent to the impact and employed to calculate maximum displacement. Cartilage degeneration was evaluated using the Mankin score.²

In Situ Impact Verification

New Zealand White female rabbits aged 18 to 24 months (retired breeders; Covance, Gaithersburg, MD) underwent nonsurvival surgery to their right knees with a medial parapatellar arthrotomy as described above. After impact,

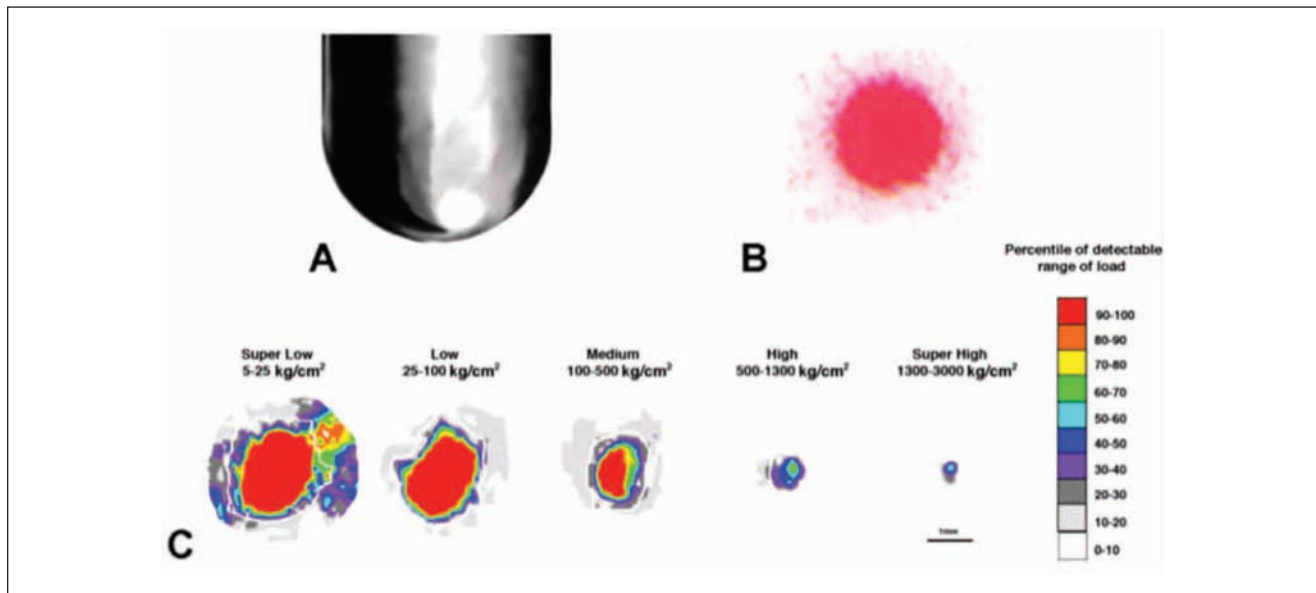


Figure 2. Hemispherical impactor tip geometry (A) and a representative Pressurex pressure-sensitive film impact pattern (B). (C) Footprints recorded with different sensitivity Pressurex pressure-sensitive films under equal loads (set to deliver 588 N [120 MPa]) as described in Materials and Methods) delivered to rabbit condyles *in situ* were calibrated and parsed in 10% increments for load (MPa).

the femoral condyles were isolated and placed in growth medium (Dulbecco's modified Eagle's medium, 10% fetal bovine serum, 3-fold penicillin/streptomycin/fungizone, and 50 mM ascorbate) for 24 hours at 37 °C. Condyles were rinsed with phosphate-buffered saline, the injuries visualized with India ink, and photographically recorded with a Qimaging Micropublisher 5.0 CCD color camera (Bumby, British Columbia, Canada) mounted on a Leica MZF1 III dissecting microscope. In a different set of experiments, isolated femoral condyles mounted in methacrylate were subjected to 5 impacts with the impactor set to the previously determined 36 MPa load level of spring compression. Each impact was monitored sequentially with pressure-sensitive paper of decreasing force sensitivity, from super low force sensitivity (5–25 kg/cm²; 0.49–2.45 MPa) to super high force sensitivity (1300–3000 kg/cm²; 127–294 MPa).

Results

Impact Characteristics

On intact articular cartilage *in vivo*, the hemispherical tip (Fig. 2A) delivered an impact with a regular shaped area ($1.39 \pm 0.11 \text{ mm}^2$; $n = 3$; Fig. 2B). The defined footprint allowed the use of the geometry of the hemispherical tip to estimate the average maximum displacement of the impactor tip into the cartilage as a result of the impact. The *in vivo* impacts measured with an internal load cell revealed a maximum force of $236 \pm 95.2 \text{ N}$ over a period of $1.5 \pm 3.1 \text{ ms}$ and $0.32 \pm 0.04 \text{ ms}$ time-to-maximum force (Table 2).

Calculation of load was based on the area of the footprint as a uniform impression, with a value of $1.39 \pm 0.11 \text{ mm}^2$, showing that the impacts delivered were $169 \pm 68.4 \text{ MPa}$. Maximal tissue displacement (strain at the apex of the tip) was calculated from the radius of the footprint and measurement of unimpacted cartilage thickness adjacent to the wound, yielding a value of $21.5\% \pm 4.5\%$.

To independently verify the internal load cell readings, Fuji Pressurex pressure-sensitive film ranging in sensitivity from 0.49 to 294 MPa (super low to super high load detection range) was laid on femoral condyles *in situ*, which were impacted as described above. Analysis of the footprints (Fig. 2C) yielded an estimated load of $330 \pm 50.3 \text{ MPa}$ from which the force of impact ($439 \pm 50.1 \text{ N}$) was calculated. Strain was calculated from the diameters of the impacts ($1.03 \pm 0.12 \text{ mm}^2$) and a mean cartilage thickness (surface to tidemark) derived from the condyles struck and analyzed in this study. Although higher than the loads reported with the internal load cell, the forces and loads reported by the Pressurex pressure-sensitive paper compared well (26% and 35% differences, respectively; Table 3).

In Vivo Impact Wound Development

We initially compared the cartilage degeneration induced by a traumatic impact versus that induced by an instability model such as ACLT and direct cartilage injury resulting from debridement by grooving (Fig. 3). Three months after injury, Safranin O/Fast Green staining of sections through the center of the area of degeneration revealed a significant difference in degree and extent of cartilage degeneration

Table 3. Comparison of Impact Parameters Measured *In Situ* Using Internal Load Cell Versus Pressure-Sensitive Film^a

Detection method	Force (N)	Absolute area (mm ²) ^b	Calculated load (MPa)	Maximum displacement (%) ^c
Internal load cell	326.9 ± 47.30	1.39 ± 0.11	212.9 ± 21.2	21.50 ± 4.50
Presssurex pressure-sensitive film	439.3 ± 50.13 ^d	1.33 ± 0.42	330.3 ± 50.3	14.23 ± 3.33 ^e

^aAll impacts generated using a blunt hemispherical tip.

^bArea determined through upper 88 % intensity (LUT function, NIH Image 1.6) of total footprint.

^cCartilage depth determined by comparison of light micrographs of impacted and neighboring unimpacted cartilage.

^dMagnitude calculated from the footprint obtained using medium-grade Presssurex pressure-sensitive film footprint.

^eBased on average lapine articular cartilage thickness in this study, 378 ± 87 μm.

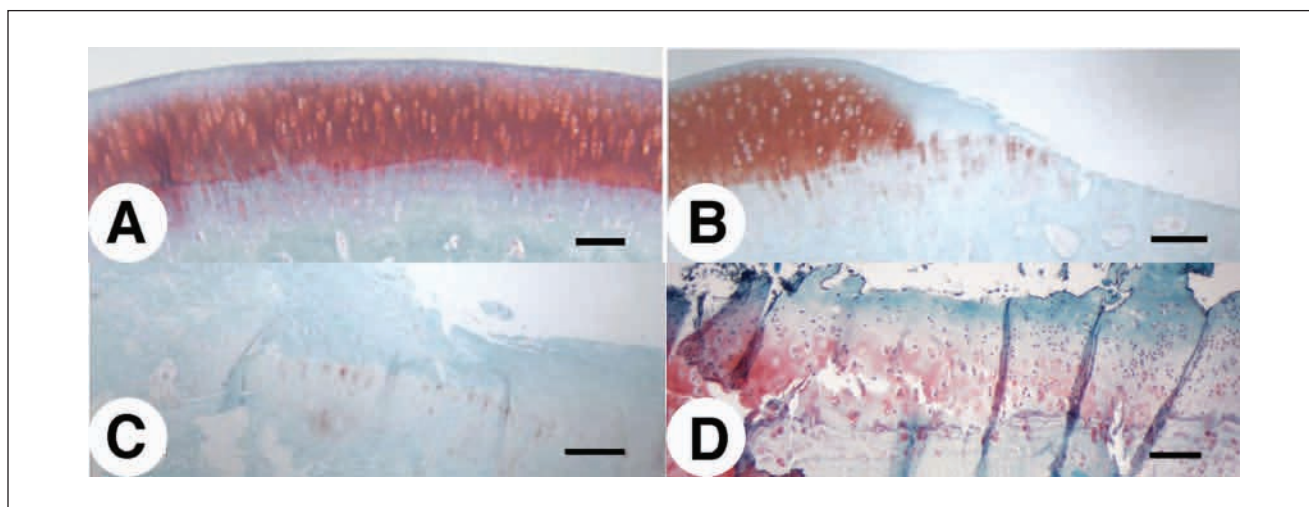


Figure 3. Comparison of cartilage damage at 12 weeks following injury onset: (A) sham control, (B) groove, (C) anterior cruciate ligament transection, and (D) impact. Sections of designated samples were stained with Safranin O for proteoglycan and with Fast Green as counter stain. Bar = 100 μm.

between these 3 models. In 12 weeks, ACLT induced rapid, widespread, and severe cartilage degeneration (Fig. 3C). Cartilage was eroded to the calcified zone, and large fibrous structures negative for proteoglycan were seen forming on the margins of the joint. In contrast, grooving induced proteoglycan and cell loss only in the margins of the defect (within 2–300 μm; Fig. 3B). Otherwise the articular cartilage appeared relatively normal. In the impact model, we observed an intermediate level of degeneration in which deep fissuring was observed, some proteoglycan and cell loss, and evidence of clonal expansion (Fig. 3D). These features are all hallmarks of osteoarthritic degeneration. Independent Mankin scores averaged between 10 and 12 in the region of the defect (data not shown).

Development of Focal Lesion Induced by *In Vivo* Impact

Twenty-four hours after impact, Safranin O/Fast Green staining of impacted articular cartilage revealed impact-induced focal damage (Fig. 4C) as compared with control

(Fig. 4A). The hemispherical tip did not penetrate the cartilage or damage the subchondral bone; however, small fissures extending into the transition zone were evident (Fig. 4C). Irregularities in the superficial zone were also evident, indicative of shear or tensile stress during the impact. At 24 hours after impact, cell loss was restricted largely to the intermediate and superficial zones (Fig. 5C) as compared with sham-operated controls (Fig. 5A). Deep zones of the articular cartilage were only mildly affected in the blunt impact.

Three months postimpact, the degenerated cartilage at the site of impact induced by the hemispherical tip had several features characteristic of advanced osteoarthritis (Fig. 4D), including erosion of the superficial zone, fissuring, overall hypocellularity, clonal expansion in specific areas, and reduction in sulfated proteoglycan content. Evidence of tidemark remodeling was also apparent. These changes were not accompanied by joint enlargement, effusion, or macroscopically observable synovial tissue growth in the time frame examined. Cell loss in the intermediate and deep zones was partial, and there was considerable clonal

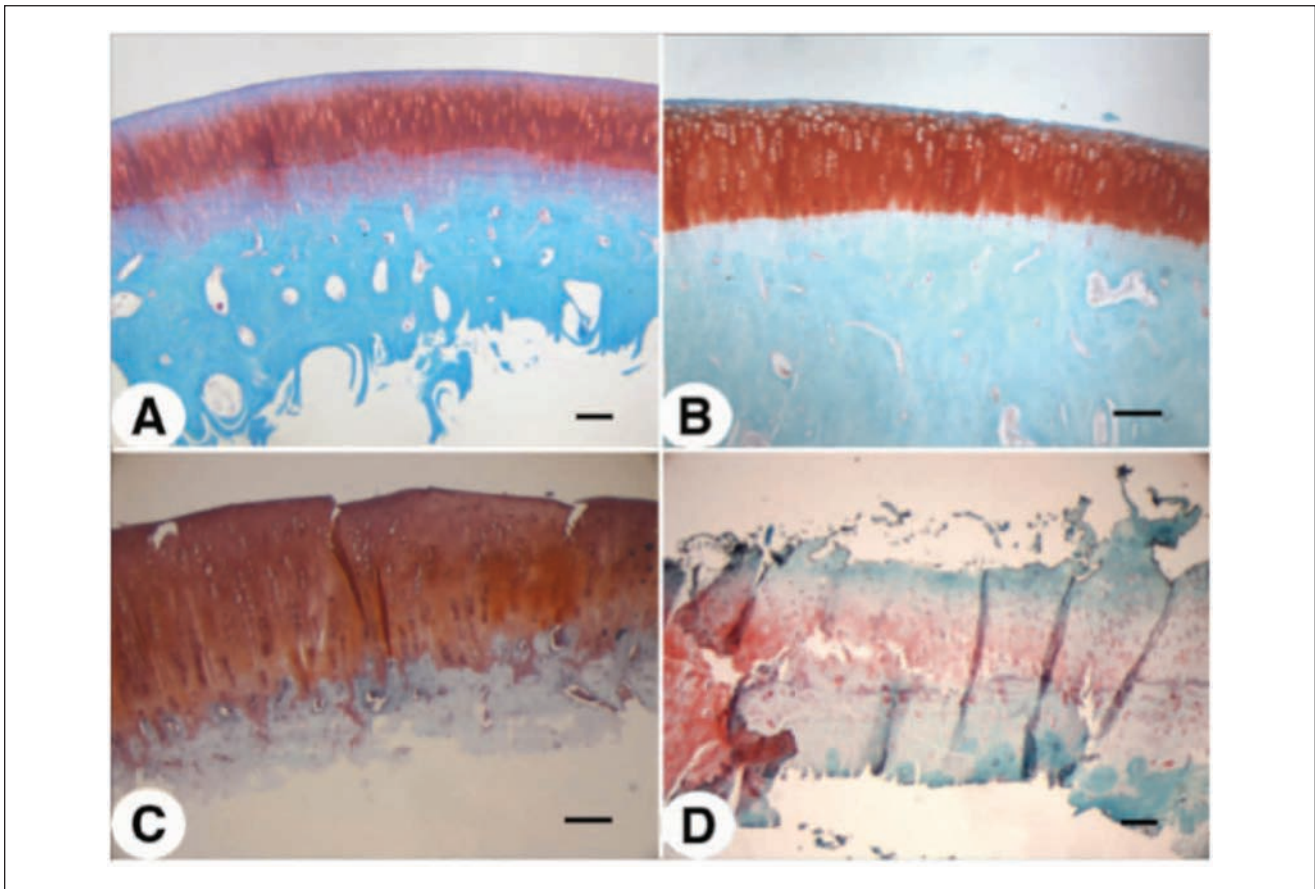


Figure 4. Histological detection of articular cartilage degeneration after impact. Sections in the impact zone of rabbit femoral chondyles were stained using Safranin O and Fast Green: (A and B) Sham-operated controls, (C and D) impacted condyles at 24 hours (A and C) and 12 weeks (B and D) after impact injury. Magnification, 4–6 \times ; scale bar = 200 μ m.

expansion among the presumed surviving cells (Fig. 5D). Quantification of cell death in the surface, intermediate and deep zones of the cartilage at 24 hours and 12 weeks after impact revealed that immediately after impact, cell death was most prominent in the surface and intermediate zones; however, by 12 weeks, the deep zone in particular lost a large percentage of cells, whereas the increase in cell death in the surface and intermediate zones was marginal or insignificant (Fig. 6). Importantly, minimal cell loss was observed in the calcified cartilage zone or in the subchondral bone. Impacted cartilage scored between 8 and 10 on the Mankin scale as compared with neighboring, unimpacted regions and unimpacted control condyles, which scored 0 or 1.

Discussion

In this report, we describe the development of an *in vivo* impact-induced model of posttraumatic osteoarthritis. At 12 weeks, the damaged areas show fracturing of the articular

cartilage extended to the tidemark, loss of sulfated proteoglycans, overall hypocellularity, and clonal cell clusters, suggesting that the mechanisms of degradation resulting from the modeled impact in this study are similar to those in clinically observed posttraumatic osteoarthritis. Furthermore, these changes occurred in the absence of observable synovitis and joint effusion characteristic of inflammatory arthritis or late-stage osteoarthritis. By definition then, this model produced primary osteoarthritis, in which damage to the articular surface initiates the disease process.

The impacts produced by the spring-loaded device are greater and faster than physiologically relevant events that include loads up to 10 to 12 MPa, and stress rates of 100 kN/s.²² Impacts mimicking traumatic events in the course of exercise and sports or major accidents (such as automobile accidents) are represented by loads of 25 to 100 MPa,^{7,23,24} although higher loads are possible in crashes exceeding 35 mph.^{25–27} Previous studies of high-intensity impacts to articular cartilage *in vivo* have employed forces of 600 to

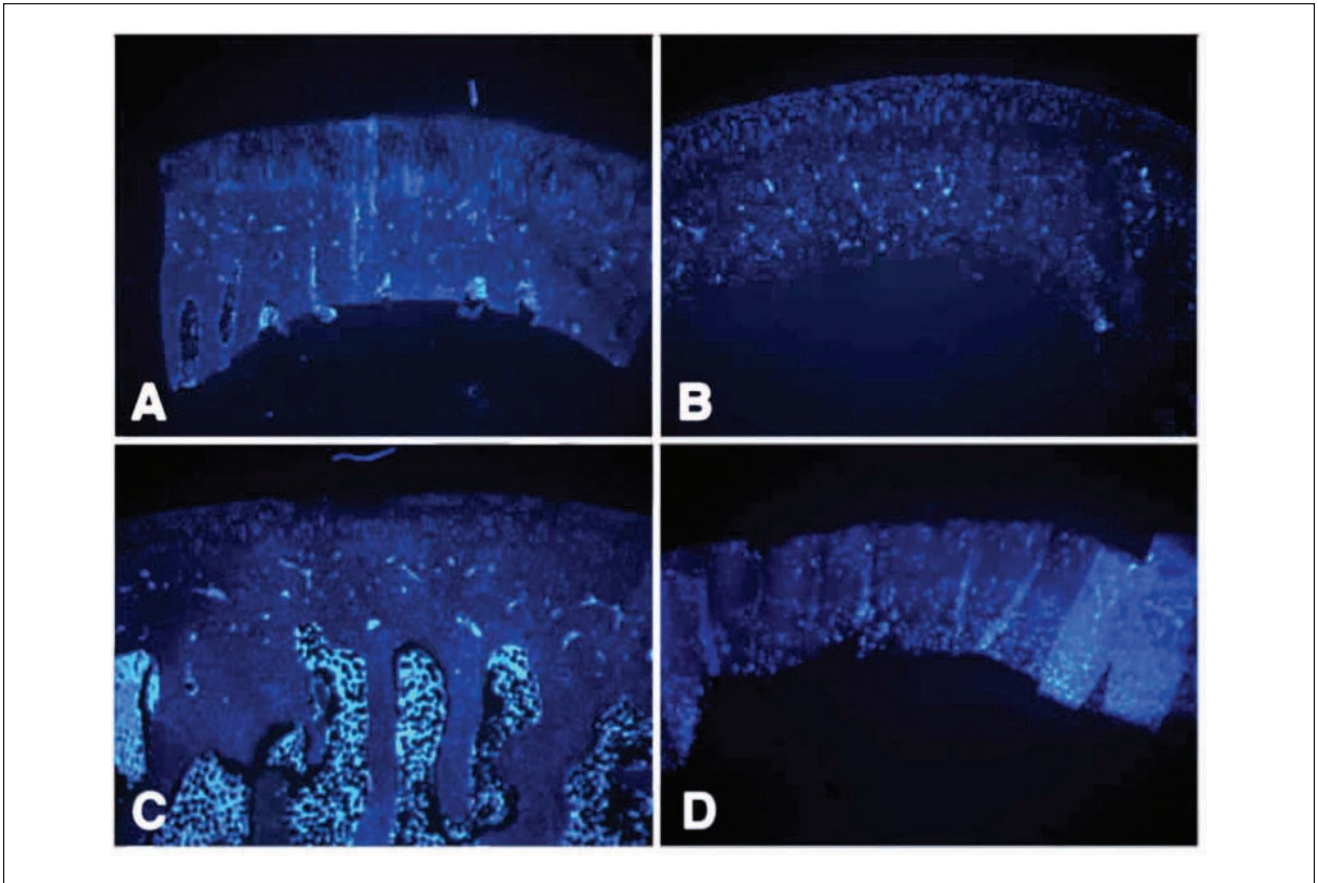


Figure 5. Cell loss in the impacted zone of articular cartilage of the rabbit femoral condyle detected by Hoechst 33342 nuclear. (A and B) Sham-operated controls, (C and D) impacted condyles at 24 hours (A and C) and 12 weeks (B and D) after impact injury. Magnification, 4–5x; scale bar = 500 μ m.

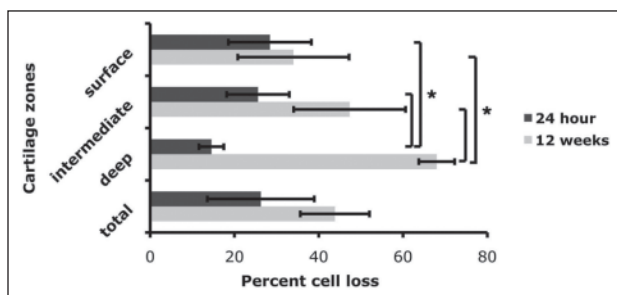


Figure 6. Quantification of cell death in impacted cartilage *in vivo*. Three sections from impacted femoral condyles at 24 hours and 12 weeks ($n = 3$ for each group) were stained with Hoechst 33342 nuclear staining. Cell loss in each zone (superficial, intermediate, and deep) of impacted cartilage is expressed as a percentage of total cell number in each zone as compared with neighboring unimpacted cartilage. Values are the mean (SD of 3 samples from one experiment (* $P < 0.01$)).

700 MPa^{24,28} or 14 to 51 MPa^{29,33} with speed or time to peak of 3.5 to 6 ms or 420 to 500 ms, respectively (Table 4). Between the impacts produced using the hemispherical tip described here and pointed tip configurations (data not shown), we measured forces between 2- and 10-fold larger than previously reported models.

The immediate damage observed 24 hours after traumatic impacts with the hemispherical tip described here is consistent with other reported studies applying impacts with similar characteristics.^{24,28} The similarities in damage include the extent and depth of fissuring and cell death patterns in relation to fissure boundaries and concentration in the transition zones.^{24,29,34,35} We observed fibrillation patterns similar to those previously documented.³⁶ The fractures initially extended into the surface and intermediate zones, at angles to the surface zone similar to collagen fibril split lines.³⁷ Studies have shown that at time to peak speeds of 100 ms or less the movement of water is inconsequential

Table 4. Summary of Reported Load Characteristics of Impacts Employed in Studies of High-Intensity Impacts *In Vivo*^a

Report	Model	Method	Load (MPa)	Duration (ms)
Atkinson et al. (2001) ³¹	Canine patellofemoral joint	Drop tower, noninvasive	44.6	5.1
Borelli et al. (2003) ³²	Rabbit femoral condyle	Pendulum, invasive	80.5	21
D'Lima et al. (2001) ³⁰	Rabbit patellofemoral joint	Drop tower, noninvasive	14.0	500
Ewers et al. (2002) ²⁸	Rabbit patellofemoral joint	Drop tower, invasive	615	4.5
Milentijevic et al. (2005) ²⁹	Rabbit femoral condyle	Pneumatic impact, invasive	40	420
Rundell et al. (2005) ²⁴	Rabbit patellofemoral joint	Drop tower, noninvasive	676.0	3.5
Zhang et al. (1999) ³³	Rabbit femoral condyle	Drop tower, noninvasive	51.8	Not reported
Current study	Rabbit femoral condyle	Spring-loaded impact, invasive	394.0	1.5

^aOnly maximum reported loads and time to peak are listed.

and cartilage ceases to act as a viscoelastic tissue.³⁶ At these impact rates, water acts increasingly as a solid, thereby more directly challenging the elastic components of the matrix. We also measured articular cartilage fractures that extended beyond the pressure-sensitive film's reported impact radius, indicating high tensile force at the surface, which are expected from the hemispherical tip.

Cell loss increased dramatically in the transition and deep zones within 24 hours after impact and clearly continued, as shown by nuclear labeling at 12 weeks.^{30,35,38} Cell death was also highest along the margins of fissures. Unlike previous studies³⁸ we did not observe high cell death in the superficial zone immediately following impact, although cell loss in this region clearly occurred as shown by the presence of a hypocellular surface zone at 12 weeks. In support of this, the characteristics of the wound produced here at 12 weeks are also similar to those described in other studies at 4 months or longer following other modalities of high-intensity traumatic impact.^{14,17,28,36,39,40} Several factors may contribute to the comparatively lower percentage of cell death observed here in the superficial zone 24 hours after impact. First, the superficial zone is adapted to tensile forces, and the cell death seen here is a testament to the high tensile forces generated by a spherical impactor. Second, the deep zone is not adapted to high tensile and shear forces, it and may be more highly susceptible to forces generated by the geometry of our impactor.

We also observed evidence of tidemark remodeling directly under the site of impact, which has been reported in some impact model studies.^{41,42} Importantly, we observed neither delamination of subchondral bone and articular cartilage nor subchondral bone fractures, which would have suggested an extreme over load of the joint tissue. The tidemark remodeling may be evidence of an altered interaction between the cartilage and bone evident at the osteochondral junction (tidemark). Communication between articular cartilage and subchondral bone has been shown in healthy cartilage, and this communication is increased in osteoarthritis.⁴³⁻⁴⁵ This remodeling may also be evidence of subchondral

bruising, an excellent indicator of cartilage damage as well.⁴⁶ The bruising can lead to subchondral bone thickening associated with osteoarthritis^{13,14,17,18,47} but is not specific to the development of osteoarthritis in animal models.^{28,41} The distinction is important because it has been hypothesized that changes in subchondral bone can drive the progression of osteoarthritis and even initiate it.⁴⁸⁻⁵² In this study, we used only a maximal impact load, which clearly fractured the cartilage and killed many cells. The impact may also have been hard enough to simultaneously bruise the bone. Importantly, we did not observe any subchondral fractures by x-ray analysis, which would have clearly complicated the model with respect to osteoarthritis progression. Future studies in which the impact load is lowered to subacute levels while specifically assaying bone health and metabolism may help elucidate the role of subchondral bone in this model.

The scope of this study did not involve a microscopic examination of the meniscus, ligaments or synovial lining. These issues are important since osteoarthritis is a disease involving tissue of the whole joint, including the synovium, meniscus, tendon, ligaments, and subchondral bone. We do report that knees of animals that underwent ACLT were swollen, exhibiting obvious synovitis and effusion, and the animals mildly favored the diseased stifle while moving. On the other hand, those with an intra-articular impact showed no apparent synovitis or effusion. This difference may be a function of different rates of disease progression in the 2 models. After 12 weeks, ACLT samples already showed extensive cartilage fibrillation and erosion to the calcified cartilage and pannus formation. In the weightbearing regions, very little cartilage tissue was evident. We classified this as advanced osteoarthritis. Because all weightbearing areas are involved in instability models, the mechanical properties that initiated the cartilage breakdown in the ACLT model were extensive enough to activate an inflammatory response in the synovial lining, inducing (presumed) inflammatory cell infiltration (resulting in synovitis), the activation of which induces the release of inflammatory mediators accelerating the loss of

cartilage and producing high joint fluid volumes (effusion). In the impact model, the initially affected area is very small. The matrix fragments and inflammatory mediators we assume are produced by the surviving chondrocytes are present and participating in the local destruction of the cartilage but are not yet released in high concentrations to activate an inflammatory response in the synovial lining. We hypothesize that if the impact model animals had been allowed to live longer, the degeneration would have proceeded and eventually the symptoms of a more global disease would become evident.

The properties and consistency of the impacting device give us confidence that we can reproducibly load the articular cartilage, estimate the magnitude of that load and, through calculation, the energy of the impact with reasonable accuracy. It is the distribution of energy and the displacement of the tissue that we cannot measure or describe here. Several factors limit our ability to measure or calculate the impact load leading to the apparent overestimation of load as compared to the wound produced *in vivo*. First, there is significant energy loss within the device itself as demonstrated using the external load cell ($19\% \pm 2\%$). Second, we recognize an unquantified loss of energy absorbed by the surrounding tissues including the subchondral bone, soft connective tissues, underlying musculature and dermis during *in vivo* impacts. After further study, a conversion factor may be used to more accurately quantify the impact. Third, the area of impact was calculated using only medium-range pressure-sensitive film, and the footprint was used as a “binomial” report of contact and force. Further experimentation and modeling of force distribution will be required to characterize the load delivered by this method. Fourth, the spherical geometry of the impactor produces force vectors that radiate perpendicularly from the tangent of the impactor tip surface, which changes for any point of the articular cartilage surface throughout the impact duration. Further modeling of force distribution will be required to quantify the force delivered by this method.

Our impactor system design described here shows promise in delivering and studying the effects of single traumatic impacts of various intensities at different locations within the joint. The wound geometry is easily adjusted by changing tips, while alteration in magnitude of impact is accomplished by a change in the properties of the springs. The calibration of the impactor *in vitro* using adult bovine articular cartilage in preparation of impacting rabbit cartilage *in vivo* was not translatable (Table 1). The two types of cartilage samples are very different in geometry and biomechanics, and the impact surface is very rigid *in vitro* even in the absence of subchondral bone, whereas *in vivo* impact surface is less rigidly secured given the soft tissue underneath the knee during impact. Optimization and calibration of the impactor must be accomplished *in situ* for each species, joint, and impact

tip. Nonetheless, this preliminary study of the *in vivo* effects of our impactor have shown that the impacts delivered are very consistent. We believe the progression of osteoarthritic degeneration in the impact model presents several opportunities. First, there is a defined area, time and mechanical insult that can be manipulated to aid in identification of critical parameters in disease initiation. Second, the pace of disease progression is slower, giving us greater opportunity to observe and assay the interactions of cartilage and bone at the tidemark, and cartilage and synovium at the level of inflammatory interactions. Third, the focal nature of the defect will allow us to test various cartilage repair modalities.

Acknowledgments

We thank Dr. John Bacher for veterinary assistance, and Dr. Wesley M. Jackson and Dr. Juan Taboas for their technical advice. Funding sources of the study include the following: Intramural Research Program of the National Institute of Arthritis, and Musculoskeletal and Skin Diseases, NIH (AR Z01 41131); Commonwealth of Pennsylvania Department of Health (SAP 4100050913); and the U.S. Department of Defense (W81XWH-10-1-0850). This research was supported by the Intramural Research Program of the National Institute of Arthritis, and Musculoskeletal and Skin Diseases, National Institutes of Health (AR Z01 41131); Commonwealth of Pennsylvania Department of Health (SAP 4100050913); and the U.S. Department of Defense (W81XWH-10-1-0850).

Declaration of Conflicting Interests

The authors declared no potential conflicts of interest with respect to the research, authorship, and/or publication of this article.

Note

Animal studies were conducted under an Institutional Animal Care and Use Committee–approved protocol.

References

1. Buckwalter JA, Saltzman C, Brown T. The impact of osteoarthritis: implications for research. *Clin Orthop Relat Res*. 2004;(427 Suppl):S6-15.
2. Mankin HJ. Biochemical and metabolic aspects of osteoarthritis. *Orthop Clin North Am*. 1971;2(1):19-31.
3. Aigner T, Kurz B, Fukui N, Sandell L. Roles of chondrocytes in the pathogenesis of osteoarthritis. *Curr Opin Rheumatol*. 2002;14(5):578-84.
4. Fukui N, Purple CR, Sandell LJ. Cell biology of osteoarthritis: the chondrocyte's response to injury. *Curr Rheumatol Rep*. 2001;3(6):496-505.
5. Goldring SR, Goldring MB. The role of cytokines in cartilage matrix degeneration in osteoarthritis. *Clin Orthop Relat Res*. 2004;(427 Suppl):S27-36.
6. Mueller MB, Tuan RS. Anabolic/catabolic balance in pathogenesis of osteoarthritis: identifying molecular targets. *PM R*. 2011;3(6 Suppl 1):S3-11.

7. Borrelli J Jr, Ricci WM. Acute effects of cartilage impact. *Clin Orthop Relat Res.* 2004;(423):33-9.
8. Vrahas MS, Mithoefer K, Joseph D. The long-term effects of articular impaction. *Clin Orthop Relat Res.* 2004;(423):40-3.
9. Brandt KD. Animal models of osteoarthritis. *Biorheology.* 2002;39(1-2):221-35.
10. van den Berg WB, van de Loo F, Joosten LA, Arntz OJ. Animal models of arthritis in NOS2-deficient mice. *Osteoarthritis Cartilage.* 1999;7(4):413-5.
11. Koh J, Dietz J. Osteoarthritis in other joints (hip, elbow, foot, ankle, toes, wrist) after sports injuries. *Clin Sports Med.* 2005;24(1):57-70.
12. Borrelli J Jr, Burns ME, Ricci WM, Silva MJ. A method for delivering variable impact stresses to the articular cartilage of rabbit knees. *J Orthop Trauma.* 2002;16(3):182-8.
13. Haut RC, Ide TM, De Camp CE. Mechanical responses of the rabbit patello-femoral joint to blunt impact. *J Biomech Eng.* 1995;117(4):402-8.
14. Newberry WN, Garcia JJ, Mackenzie CD, Decamp CE, Haut RC. Analysis of acute mechanical insult in an animal model of post-traumatic osteoarthrosis. *J Biomech Eng.* 1998;120(6):704-9.
15. Torzilli PA, Grigiene R, Borrelli J Jr, Helfet DL. Effect of impact load on articular cartilage: cell metabolism and viability, and matrix water content. *J Biomech Eng.* 1999;121(5):433-41.
16. Vrahas MS, Smith GA, Rosler DM, Baratta RV. Method to impact *in vivo* rabbit femoral cartilage with blows of quantifiable stress. *J Orthop Res.* 1997;15(2):314-7.
17. Newberry WN, Zukosky DK, Haut RC. Subfracture insult to a knee joint causes alterations in the bone and in the functional stiffness of overlying cartilage. *J Orthop Res.* 1997;15(3):450-5.
18. Radin EL, Paul IL, Pollock D. Animal joint behaviour under excessive loading. *Nature.* 1970;226(5345):554-5.
19. Kerin A, Patwari P, Kuettner K, Cole A, Grodzinsky A. Molecular basis of osteoarthritis: biomechanical aspects. *Cell Mol Life Sci.* 2002;59(1):27-35.
20. Moskowitz RW, Davis W, Sammarco J, Martens M, Baker J, Mayor M, *et al.* Experimentally induced degenerative joint lesions following partial meniscectomy in the rabbit. *Arthritis Rheum.* 1973;16(3):397-405.
21. Marijnissen AC, van Roermund PM, TeKoppele JM, Bijlsma JW, Lafeber FP. The canine 'groove' model, compared with the ACLT model of osteoarthritis. *Osteoarthritis Cartilage.* 2002;10(2):145-55.
22. Aspden RM, Jeffrey JE, Burgin LV. Impact loading of articular cartilage. *Osteoarthritis Cartilage.* 2002;10(7):588-9.
23. Robinovitch SN, Chiu J. Surface stiffness affects impact force during a fall on the outstretched hand. *J Orthop Res.* 1998;16(3):309-13.
24. Rundell SA, Baars DC, Phillips DM, Haut RC. The limitation of acute necrosis in retro-patellar cartilage after a severe blunt impact to the *in vivo* rabbit patello-femoral joint. *J Orthop Res.* 2005;23(6):1363-9.
25. Cheng R, Yang K-H, Levine RS, King AI. Dynamic impact loading of the femur under passive restrained loading. In: *Proceedings of the 28th Stapp Car Crash Conference; 1984 Nov 6-7; Chicago, IL. Warrendale, PA: Society of Automotive Engineers; 1984. p. 101-18.*
26. Kroell CK, Schneider DC. Comparative knee impact response of 572 dummy and cadaver subjects. In: *Proceedings of the 20th Stapp Car Crash Conference; 1976 Oct 18-20; Dearborn, MI. Warrendale, PA: Society of Automotive Engineers; 1976. p. 237-59.*
27. Patrick LM, Kroell CK, Wirth CR. Forces on the human body in simulated crashes. In: *Proceedings of the 9th Stapp Car Crash Conference; 1965. Warrendale, PA: Society of Automotive Engineers; 1966. p. 237-59.*
28. Ewers BJ, Weaver BT, Sevensma ET, Haut RC. Chronic changes in rabbit retro-patellar cartilage and subchondral bone after blunt impact loading of the patellofemoral joint. *J Orthop Res.* 2002;20(3):545-50.
29. Milentijevic D, Rubel IF, Liew AS, Helfet DL, Torzilli PA. An *in vivo* rabbit model for cartilage trauma: a preliminary study of the influence of impact stress magnitude on chondrocyte death and matrix damage. *J Orthop Trauma.* 2005;19(7):466-73.
30. D'Lima DD, Hashimoto S, Chen PC, Colwell CW Jr, Lotz MK. Impact of mechanical trauma on matrix and cells. *Clin Orthop Relat Res.* 2001;(391 Suppl):S90-9.
31. Atkinson, PJ, Haut, RC. Injuries produced by blunt trauma to the human patellofemoral joint vary with flexion angle of the knee. *J Orthop Res.* 2001;19(5):827-33.
32. Borelli, J, Tinsley, K, Ricci, WM, Burns, M, Karl, IE, Hotchkiss, R. Induction of chondrocyte apoptosis following impact load. *J Orthop Trauma.* 2003;17(9):635-41.
33. Zhang, H, Vrahas, MS, Baratta, RV, Rosler, DM. Damage to rabbit femoral cartilage following direct impact of uniform stresses: an *in vitro* study. *Clin Biomech.* 1999;14(8):543-8.
34. Ewers BJ, Dvoracek-Driksna D, Orth MW, Haut RC. The extent of matrix damage and chondrocyte death in mechanically traumatized articular cartilage explants depends on rate of loading. *J Orthop Res.* 2001;19(5):779-84.
35. Lewis JL, Deloria LB, Oyen-Tiesma M, Thompson RC Jr, Ericson M, Oegema TR Jr. Cell death after cartilage impact occurs around matrix cracks. *J Orthop Res.* 2003;21(5):881-7.
36. Ewers BJ, Jayaraman VM, Banglmaier RF, Haut RC. Rate of blunt impact loading affects changes in retropatellar cartilage and underlying bone in the rabbit patella. *J Biomech.* 2002;35(6):747-55.
37. Jeffrey JE, Gregory DW, Aspden RM. Matrix damage and chondrocyte viability following a single impact load on articular cartilage. *Arch Biochem Biophys.* 1995;322(1):87-96.
38. Kuhn K, D'Lima DD, Hashimoto S, Lotz M. Cell death in cartilage. *Osteoarthritis Cartilage.* 2004;12(1):1-16.

39. Lukoschek M, Boyd RD, Schaffler MB, Burr DB, Radin EL. Comparison of joint degeneration models. Surgical instability and repetitive impulsive loading. *Acta Orthop Scand*. 1986;57(4):349-53.
40. Thompson RC Jr, Oegema TR Jr, Lewis JL, Wallace L. Osteoarthrotic changes after acute transarticular load. An animal model. *J Bone Joint Surg Am*. 1991;73(7):990-1001.
41. Ewers BJ, Newberry WN, Haut RC. Chronic softening of cartilage without thickening of underlying bone in a joint trauma model. *J Biomech*. 2000;33(12):1689-94.
42. Newberry WN, Mackenzie CD, Haut RC. Blunt impact causes changes in bone and cartilage in a regularly exercised animal model. *J Orthop Res*. 1998;16(3):348-54.
43. Pan J, Wang B, Li W, Zhou X, Scherr T, Yang Y, *et al*. Elevated cross-talk between subchondral bone and cartilage in osteoarthritic joints. *Bone*. Epub 2011 Dec 6.
44. Fetter NL, Leddy HA, Guilak F, Nunley JA. Composition and transport properties of human ankle and knee cartilage. *J Orthop Res*. 2006;24(2):211-9.
45. Botter SM, van Osch GJ, Clockaerts S, Waarsing JH, Weinans H, van Leeuwen JP. Osteoarthritis induction leads to early and temporal subchondral plate porosity in the tibial plateau of mice: an *in vivo* microfocal computed tomography study. *Arthritis Rheum*. 2011;63(9):2690-9.
46. Johnson DL, Urban WP Jr, Caborn DN, Vanarthos WJ, Carlson CS. Articular cartilage changes seen with magnetic resonance imaging-detected bone bruises associated with acute anterior cruciate ligament rupture. *Am J Sports Med*. 1998;26(3):409-14.
47. Radin EL, Parker HG, Pugh JW, Steinberg RS, Paul IL, Rose RM. Response of joints to impact loading. 3. Relationship between trabecular microfractures and cartilage degeneration. *J Biomech*. 1973;6(1):51-7.
48. Suri S, Walsh DA. Osteochondral alterations in osteoarthritis. *Bone*. Epub 2011 Oct 17.
49. Brandt KD, Radin EL, Dieppe PA, van de Putte L. Yet more evidence that osteoarthritis is not a cartilage disease. *Ann Rheum Dis*. 2006;65(10):1261-4.
50. Lories RJ, Luyten FP. The bone-cartilage unit in osteoarthritis. *Nat Rev Rheumatol*. 2011;7(1):43-9.
51. Bellido M, Lugo L, Roman-Blas JA, Castaneda S, Calvo E, Largo R, *et al*. Improving subchondral bone integrity reduces progression of cartilage damage in experimental osteoarthritis preceded by osteoporosis. *Osteoarthritis Cartilage*. 2011;19(10):1228-36.
52. Lahm A, Uhl M, Erggelet C, Haberstroh J, Mrosek E. Articular cartilage degeneration after acute subchondral bone damage: an experimental study in dogs with histopathological grading. *Acta Orthop Scand*. 2004;75(6):762-7.